Immuno-PET Detects Antibody–Drug Potency on Coadministration with Statins

Emma L. Brown*[1], Shayla Shmuel*[1], Komal Mandleywala*[2], Sandeep Surendra Panikar[1], Na-Keysha Berry[1], Yi Rao[2], Abbey Zidel[1,3], Jason S. Lewis[2,4–7], and Patrícia M.R. Pereira[1]

[1]*Department of Radiology, Mallinckrodt Institute of Radiology, Washington University School of Medicine, St. Louis, Missouri;* [2]*Department of Radiology, Memorial Sloan Kettering Cancer Center, New York, New York;* [3]*Department of Biology, Washington University School of Medicine, St. Louis, Missouri;* [4]*Department of Pharmacology, Weill Cornell Medical College, New York, New York;* [5]*Molecular Pharmacology Program, Memorial Sloan Kettering Cancer Center, New York, New York;* [6]*Department of Radiology, Weill Cornell Medical College, New York, New York; and* [7]*Radiochemistry and Molecular Imaging Probes Core, Memorial Sloan Kettering Cancer Center, New York, New York*

The human epidermal growth factor receptor 2 (HER2)–targeting trastuzumab emtansine (T-DM1) and trastuzumab deruxtecan (T-DXd) are antibody–drug conjugates (ADC) clinically used to treat HER2-positive breast cancer, with the latter receiving clinical approval in 2021 for HER2-positive gastric cancer. Lovastatin, a cholesterol-lowering drug, temporally elevates cell-surface HER2 in ways that enhance HER2-ADC binding and internalization. **Methods:** In an NCIN87 gastric xenograft model and a gastric patient–derived xenograft model, we used the ^{89}Zr-labeled or ^{64}Cu-labeled anti-HER2 antibody trastuzumab to investigate the dosing regimen of ADC therapy with and without coadministration of lovastatin. We compared the ADC efficacy of a multiple-dose ADC regime, which replicates the clinical dose regimen standard, with a single-dose regime. **Results:** T-DM1/lovastatin treatment inhibited tumor growth, regardless of multiple- or single-dose T-DM1 administration. Coadministration of lovastatin with T-DM1 or T-DXd as a single dose enhanced tumor growth inhibition, which was accompanied by a decrease in signal on HER2-targeted immuno-PET and a decrease in HER2-mediated signaling at the cellular level. DNA damage signaling was increased on ADC treatment in vitro. **Conclusion:** Our data from a gastric cancer xenograft show the utility of HER2-targeted immuno-PET to inform the tumor response to ADC therapies in combination with modulators of cell-surface target availability. Our studies also demonstrate that statins enhance ADC efficacy in both a cell-line and a patient-derived xenograft model in ways that enable a single-dose administration of the ADC.

Key Words: ADC; T-DM1; T-DXd; PET imaging

J Nucl Med 2023; 64:1638–1646
DOI: 10.2967/jnumed.122.265172

Treatment of human epidermal growth factor receptor 2 (HER2)–expressing metastatic breast cancer has been greatly improved using trastuzumab (*1*), an antibody targeting membrane HER2. In addition to trastuzumab, antibody–drug conjugates (*2,3*) (ADCs) enable a potent chemotherapeutic payload to be delivered directly to the tumor tissue (*4–6*). Examples of ADCs targeted toward HER2 include trastuzumab emtansine (T-DM1) and trastuzumab deruxtecan (T-DXd) (*6–8*).

HER2 is a potential therapeutic target not only in breast cancer but also in other HER2-expressing solid tumors, including those of the lung, bladder, and stomach (*3,5,7,9–12*). HER2 is overexpressed in approximately 20% of metastatic gastric cancers (*13*), and similar to HER2-positive breast cancer, adding chemotherapy to trastuzumab improved survival in the first-line metastatic setting in patients with gastric cancer (*14*). However, contrary to breast cancer, no improvement in overall survival was observed in patients with gastric cancer treated with T-DM1 (7.9 mo) versus taxane (8.6 mo) (*15*). Until recently, there was a lack of meaningful clinical response of HER2-targeted agents in treating gastric cancer. However, the latest results with T-DXd in HER2-low and HER2-high tumors brought a paradigm shift (*6*). T-DXd became Food and Drug Administration–approved in 2021 for treating patients with HER2-positive gastric cancer. T-DXd has also shown efficacy in HER2-low gastric tumors (ClinicalTrials.gov identifier NCT04379596) (*16*), with an objective response rate of up to 26.3% (*17*).

For T-DM1 and T-DXd to bind to tumors, the HER2 receptor must be available at the cancer cell membrane (*4*). However, gastric tumors are characterized by a heterogeneous expression of HER2 and nonpredominant staining of HER2 at the cell membrane that impairs antibody binding to tumors (*11,13,18*). Importantly, HER2 heterogeneity is associated with resistance to HER2-targeted therapies (*19*). HER2 membrane availability is in part regulated by caveolae-mediated endocytosis, which is often dysregulated in cancer cells, resulting in heterogeneous HER2 membrane expression, particularly in gastric cancer (*18,20*).

Statins are pharmacologic inhibitors of endocytosis, likely via temporal depletion of cholesterol (*21,22*). Lovastatin is a statin prodrug that is enzymatically hydrolyzed in the liver to its active form, which inhibits 3-hydroxy-3-methylglutaryl coenzyme A, a key enzyme in the mevalonate pathway that produces isoprene moieties needed for cholesterol biosynthesis (*23,24*). Lovastatin modulates endocytosis to increase cell-surface HER2 availability, resulting in increased antibody–tumor binding (*18*). Lovastatin increased T-DM1 efficacy in gastric tumor xenografts and a patient-derived xenograft (PDX) model from a gastric tumor resistant to anti-HER2 therapy in the clinic (*21*). In this previous study, mice were administered weekly doses of T-DM1, mimicking existing clinical dose regimes.

Received Nov. 16, 2022; revision accepted May 12, 2023.
For correspondence or reprints, contact Patrícia M.R. Pereira (ribeiropereirap@wustl.edu).
*Contributed equally to this work.
Published online Jun. 29, 2023.

Although using T-DM1 and T-DXd significantly increases the overall survival of some patients, clinical trials using multiple doses of T-DM1 and T-DXd have noted some significant side effects. T-DM1 causes cardiotoxicity in approximately 3.37% of breast cancer patients (*25*), whereas early clinical data on gastric cancer suggest that 10% of T-DXd–treated patients develop interstitial lung disease (*17*). These toxicities limit the number of dosing cycles that patients can tolerate and can result in dose reductions or termination of the treatment (*17,26*). Strategies that reduce toxic side effects caused by ADCs and predictive biomarkers of ADC toxicity are a currently unmet clinical need.

Therefore, this study had 2 objectives. The first was to determine whether a single dose of ADCs could be administered in combination with lovastatin to achieve therapeutic efficacy similar to that of a multiple-dose ADC regime in both a HER2-positive xenograft and PDX gastric cancer models of known resistance to anti-HER2 therapy. The second was to use HER2-targeted immuno-PET to monitor changes in HER2 expression after ADC therapy.

MATERIALS AND METHODS

Cell Culture and Treatments

The human gastric cancer cell line NCIN87 was purchased from the American Type Culture Collection. NCIN87 were cultured in RPMI 1640 growth medium supplemented with 10% fetal calf serum, 2 mM L-glutamine, 10 mM hydroxyethyl piperazineethanesulfonic acid, 1 mM sodium pyruvate, 4,500 mg L^{-1} glucose, 1,500 mg L^{-1} sodium bicarbonate, and 100 units mL^{-1} penicillin and streptomycin.

NCIN87 cells were treated with vehicle, T-DM1, or T-DXd for 48 h before lysates were extracted. Cells additionally given lovastatin were incubated with 25 μM of the active form of lovastatin (Millipore) for 4 h before addition of T-DM1 or T-DXd.

Western Blot Analysis

Total protein extracts from NCIN87 cells and tumors were prepared after tissue homogenization in radioimmunoprecipitation assay buffer (150 mM sodium chloride, 50 mM Tris hydrochloride, pH 7.5, 5 mM ethylene glycol tetraacetic acid, 1% Triton X-100 [Dow], 0.5% sodium deoxycholate, 0.1% sodium dodecyl sulfate, 2 mM phenylmethanesulfonyl, 2 mM iodoacetamide, and ×1 protease inhibitor cocktail [Roche]). After centrifugation at 18,000*g* for 16 min at 4°C, supernatants containing total protein extracts were collected and stored at −80°C. The amount of total protein in tumor extracts was quantified using the Pierce bicinchoninic acid protein assay kit (Thermo Fisher Scientific), followed by denaturation of the sample with NuPAGE lithium dodecyl sulfate sample buffer and NuPAGE sample reducing agent (Thermo Fisher Scientific). The denatured samples underwent gel electrophoresis and transfer to polyvinylidene difluoride membranes (Bio-Rad). The membranes were incubated in 5% (m/v) milk (Bio-Rad) or bovine serum albumin (Sigma) in tris-buffered saline buffer-polysorbate (EZ BioResearch). The membranes were then incubated with the primary antibodies: mouse anti-β-actin, 1:10,000 (A1978; Sigma); rabbit anti-HER2, 1:800 (ab131490; Abcam); rabbit anti-HER2 phospho Y1139, 1:500 (ab53290; Abcam); rabbit anti–epidermal growth factor receptor (EGFR), 1:1,000 (ab52894; Abcam); rabbit anti-EGFR phospho Y1068, 1:500 (ab40815; Abcam); rabbit anti-HER3, 1:500 (ab32121; Abcam); rabbit anti-HER3 phospho Y1289, 1:2,500 (ab76469; Abcam); mouse antiphosphotyrosine, 1:2,000 (05-321; Sigma); rabbit anti–poly(adenosine diphosphate ribose) polymerase (PARP), 1:1,000 (9542; Cell Signaling Technology); rabbit anti–histone H2A.X, 1:1,000 (2595; Cell Signaling Technology); or rabbit anti–phosphohistone H2A.X (Ser139), 1:1,000 (9718; Cell Signaling Technology). After washing of the membranes with tris-buffered saline buffer-polysorbate, the membranes were incubated with the secondary antibody goat anti-rabbit IgG (heavy- and light-chain) conjugated with AlexaFluor Plus 680 (Invitrogen) or goat anti-mouse IgG (heavy- and light-chain) conjugated with AlexaFluor Plus 800 (Invitrogen). Membranes were imaged on an Odyssey infrared imaging system (LI-COR Biosciences), and densiometric analysis of the respective bands was performed using ImageJ/FIJI. The supplemental materials (available at http://jnm.snmjournals.org) contain uncropped scans of the blots shown in the figures.

Conjugation and Radiolabeling of Trastuzumab

Trastuzumab (Herceptin; Roche) used in imaging and biodistribution studies was obtained from the Siteman Cancer Center pharmacy or the Memorial Sloan Kettering pharmacy.

^{89}Zr-Labeled Trastuzumab. As previously described (*18,21*), conjugation and radiolabeling of trastuzumab with zirconium-89 were achieved using the bifunctional chelate *p*-isothiocyanatobenzyl-desferrioxamine (DFO-Bz-NCS; Macrocyclics, Inc). [^{89}Zr]Zr-oxalate was obtained from the cyclotron at Memorial Sloan Kettering Cancer Center. The ^{89}Zr-labeled trastuzumab used in our studies had a radiochemical purity of 99% as determined by instant thin-layer chromatography, and the molar activity was 21.98 MBq/nmol.

^{64}Cu-Labeled Trastuzumab. Copper-64 was obtained from Washington University Cyclotron facility. Trastuzumab was buffer-exchanged in 0.1 M 4-(2-hydroxyethyl)-1-piperazineethanesulfonic acid buffer (pH 8.5) and was conjugated and radiolabeled as previously described (*27*). Briefly, conjugation and radiolabeling of trastuzumab with copper-64 were achieved by conjugating trastuzumab to *p*-SCN-Bn-NOTA (Macrocyclics) in 100% ethanol in a 20-fold molar excess, before incubation at 4°C overnight with slow agitation. The antibody–NOTA conjugate was purified and concentrated in 0.1 M ammonium acetate buffer (pH 6) and then radiolabeled with copper-64. The reaction mixture was incubated at 37°C for 1 h. The radiochemical yield and purity were determined as described above in a mixture of 0.1 M ammonium acetate buffer (pH 6) with 50 mM ethylenediaminetetraacetic acid as the mobile phase. The radiolabeled conjugates used for in vivo studies had a radiochemical purity of 99%, radiochemical yields ranging from 87% to 99%, and molar activities in the range of 47.4–69.6 MBq/nmol.

Tumor Xenografts and Animal Studies

The animal experiments were conducted at both Washington University in St. Louis and Memorial Sloan Kettering Cancer Center. All animals were treated according to the guidelines approved by the Research Animal Resource Center and Institutional Animal Care and Use Committee at Washington University School of Medicine at St. Louis or the Research Animal Resource Center and Institutional Animal Care and Use Committee at Memorial Sloan Kettering Cancer Center.

NCIN87 Gastric Xenografts. Eight- to 10-wk-old *nu/nu* female mice (Charles River Laboratories) were injected subcutaneously on the right shoulder with 5 million NCIN87 cells in a 200-μL cell suspension of a 1:1 (v/v) mixture of Matrigel (BD Biosciences). The mice were housed in type II polycarbonate cages, fed with a sterilized standard laboratory diet, and given sterile water ad libitum. The animals were housed at approximately 19°C–23°C, at 30%–70% relative humidity, and in a 12 h light/12 h dark cycle.

The tumor volume (V/mm^3) was estimated by external vernier caliper measurements of the longest axis, a/mm, and the axis perpendicular to the longest axis, b/mm. The tumors were assumed to be spheroid, and the volume was calculated in accordance with the equation $V = (4\pi/3) \times (a/2)^2 \times (b/2)$.

PDXs. A gastric PDX model was established by the Antitumor Assessment Core at Memorial Sloan Kettering Cancer Center from a patient with HER2-positive gastric cancer, collected under an approved institutional review board protocol by the Research Animal Resource Center and Institutional Animal Care and Use Committee at Memorial

Sloan Kettering Cancer Center. Tumor fragments were mixed with Matrigel and implanted subcutaneously in 6- to 8-wk-old female NSG mice (Jackson Laboratories). Once established, tumors were maintained and expanded by serial subcutaneous transplantation. Tumor samples were evaluated as described previously (*21*), to grade for HER2 expression and to exclude B-cell lymphomas in PDXs associated with Epstein–Barr virus.

In Vivo Therapeutic Efficacy

When tumor volumes reached approximately 200–500 mm^3, mice were randomly grouped into treatment cohorts (≥8 per group for T-DM1 treatments and ≥5 per group for T-DXd treatments). Supplemental Table 1 outlines the therapeutic studies conducted, the number of animals per group, and the imaging agents used.

Multiple-Treatment T-DM1 Schedule. The multiple-treatment schedule was published previously (*21*). Vehicle, T-DM1, lovastatin, or a combination of T-DM1 with lovastatin was administered to mice bearing NCIN87 or gastric PDX tumors. Intravenous T-DM1 administration was 5 mg/kg (once weekly, for 5 wk). Lovastatin (4.15 mg/kg, oral gavage) was administrated 12 h before and at the same time as the intravenous injection of T-DM1. Tumor volumes were determined by vernier caliper measurement twice a week.

Single-Treatment T-DM1 Schedule. A single dose of vehicle or T-DM1, 5 mg/kg, was administered, and tumor volumes were measured as described above. In cohorts of T-DM1 single-dose treatment combined with lovastatin, the lovastatin (4.15 mg/kg, oral gavage) was administrated 12 h before and at the same time as the intravenous injection of T-DM1.

T-DXd Treatment. Vehicle, T-DXd, or a combination of T-DXd with lovastatin was administered to mice bearing NCIN87 or gastric PDX tumors. The mice received an intravenous injection of T-DXd (5 mg/kg, single-dose). Lovastatin (4.15 mg/kg, oral gavage) was administrated 12 h before and at the same time as the intravenous injection of T-DXd. Tumor volumes were determined by vernier caliper measurement twice a week.

Acute Biodistribution Studies and Small-Animal PET

Supplemental Table 1 outlines the imaging agents used in each treatment cohort. Mice in the T-DM1/statin cohorts were administered ^{89}Zr-labeled trastuzumab on day 39 after initiating therapy. Acute biodistribution studies were performed 48 h after injection of radiolabeled [^{89}Zr]Zr-DFO-trastuzumab. The mice were sacrificed and organs were harvested and measured in the γ-counter. Radioactivity associated with each organ was expressed as percentage injected dose per gram of organ (%ID/g).

Mice in the T-DXd/statin cohorts were administered ^{64}Cu-labeled trastuzumab before initiating therapy or on day 29 after therapy.

PET imaging experiments at Memorial Sloan Kettering were conducted on a microPET Focus 120 scanner (Concorde Microsystems) at 48 h after intravenous injection of [^{89}Zr]Zr-DFO-trastuzumab. The mice were anesthetized by inhalation of 1.5%–2% isoflurane (Baxter Healthcare) in an oxygen gas mixture 10 min before recording PET images. PET data for each group ($n = 4$) were recorded with the mice under isoflurane anesthesia (1.5%–2%). Images were analyzed using ASIPro VM software (Concorde Microsystems).

PET imaging experiments at Washington University in St. Louis were conducted on a Mediso nanoScan PET/CT scanner (Mediso) at 24 h after injection of [^{64}Cu]Cu-NOTA-trastuzumab. PET images for each group ($n = 2$) were collected before therapy and on day 30 after therapy and were recorded with the mice under isoflurane anesthesia (1.5%–2%) as described above. Images were reviewed using 3D Slicer software (version 5.0.3).

Statistical Analysis

Data were analyzed using RStudio and GraphPad Prism, version 9.0. The volume fold-change for each tumor was calculated as the tumor volume at the endpoint (mm^3) divided the tumor volume at the start of therapy (mm^3). Differences in fold-change were analyzed by a 1-way ANOVA or an unpaired Student *t* test. Differences in tumor volume over time between treatment groups were calculated using a 2-way repeated-measures ANOVA. Mean activity in the tumor region of interest (%ID/g) was quantified using 3D Slicer, version 5.2.2. The correlation between mean %ID/g and tumor volume was calculated by the Pearson correlation coefficient.

RESULTS

A Single Dose of T-DM1 Combined with Statin Reduces Tumor Volume in Gastric Cancer Xenografts

Previous work has shown that statins enhanced trastuzumab accumulation in tumors (*18*) and that coadministration of the anti-HER2 ADC T-DM1 with statins enhanced efficacy in gastric cancer mouse models in a multiple-dose T-DM1 treatment regime that mimicked the weekly infusion schedules performed in clinics (*21*). In these previous studies, a multiple-dose regime of 5 weekly 5 mg/kg doses of T-DM1 was administered in combination with a 4.15 mg/kg dose of lovastatin administered twice, 12 h before and on the day of T-DM1 administration. This multiple-dose ADC regime significantly reduced NCIN87 tumor volumes compared with T-DM1 alone, statin alone, or control saline-treated tumor cohorts (*21*). Because of the possible side effects that a multiple-dose infusion schedule of T-DM1 can cause (*25*), we sought to investigate whether the enhanced potency of T-DM1 seen on coadministration with statins could enable fewer doses of T-DM1 to be given, without interfering with therapeutic efficacy.

We first determined whether using T-DM1/statin as a single dose effectively treated NCIN87 gastric tumor xenografts (Figs. 1A and 1B). In our current study, a single 5 mg/kg dose of T-DM1 was administered, with a 4.15 mg/kg dose of lovastatin administered twice. As performed in our previous studies, the statin was administered 12 h before and on the day of T-DM1 administration. NCIN87 tumor volumes monitored across a 60 d period from treatment initiation were significantly lower ($P < 0.001$) in T-DM1/statin cohorts, even with single-dose T-DM1 administration, than with control and T-DM1 administration alone (Fig. 1B; Supplemental Fig. 1). Both T-DM1/statin cohorts had a significantly lower ($P < 0.001$) tumor volume fold-change than the T-DM1–alone equivalent in both single- and multiple-dose regimes (Fig. 1C). The tumor volume fold-change was significantly lower ($P < 0.001$) in T-DM1/statin cohorts in a multiple-dose regime than in a single-dose regime (Fig. 1C).

Overall, we found that a single dose of T-DM1, when combined with a statin, controlled NCIN87 gastric xenografts over a period of 60 d.

PET Imaging Annotates Alterations in Tumoral HER2 in Response to T-DM1/statin Combination

Noninvasive PET imaging using [^{89}Zr]Zr-DFO-trastuzumab can annotate changes in HER2 expression in response to HER2-targeted therapies (*18,21*). Therefore, we next sought to determine whether PET imaging could visualize changes in HER2 tumoral expression accompanying the decrease in tumor volume in T-DM1–treated or T-DM1/statin-treated NCIN87 xenograft tumors.

[^{89}Zr]Zr-DFO-trastuzumab was injected at 39 d after treatment initiation, the time at which NCIN87 tumors develop resistance to weekly doses of T-DM1 (*21*). In our experiments, the radiolabeled trastuzumab binds to tumoral membrane HER2 in vivo, and PET images are acquired at 48 h after antibody injection. On the basis of data shown in Figure 1, we expected that a decrease in tumor

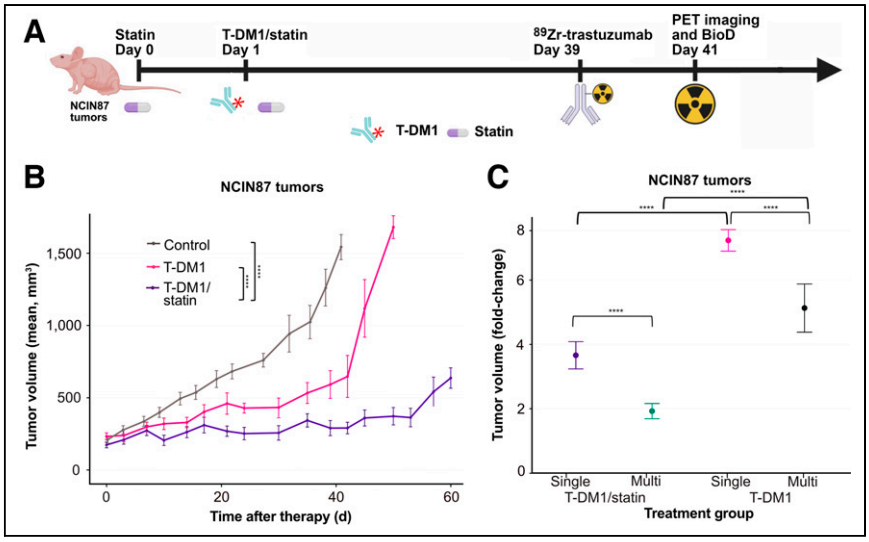

FIGURE 1 (A) Schematic illustrating T-DM1 and statin dose administration in single-dose ADC regime. NCIN87 gastric xenografts were established in female nude mice (≥8 per group). Once tumors reached 200–300 mm^3, intravenous T-DM1 administration at 5 mg/kg weekly (for 1 wk—single-treatment regime) was started on day 1. Lovastatin (4.15 mg/kg) was orally administered 12 h before and simultaneously with intravenous injection of T-DM1. [^{89}Zr]Zr-DFO-trastuzumab was intravenously administered on day 39, and PET images were collected at 41 d after treatment. Immediately after PET imaging, organs were harvested for ex vivo biodistribution. Tumors were excised at 43 d after initiating therapy and used for Western blot analyses. Schematic was created with Biorender.com. (B) Tumor volumes (mm^3) measured across 60 d for control, T-DM1 single-treatment regime, and T-DM1/statin single-treatment regime. Mean ± SD for at least 8 mice is shown. ****$P < 0.0001$ based on 2-way repeated measures ANOVA. (C) Fold-change in NCIN87 tumor volume for T-DM1 or T-DM1/statin (1 wk of therapy, single-treatment regime) and for T-DM1 or T-DM1/statin (5 wk, multiple-treatment regime reported (*21*)). Fold-change between day 0 and day 60 is displayed as mean ± SD ($n \geq 8$). ****$P < 0.0001$ based on 1-way ANOVA.

volume observed in T-DM1/statin cohorts would be accompanied by a reduction in HER2 expression as monitored by HER2-targeted immuno-PET. Immuno-PET after ADC therapy demonstrated decreased uptake of [^{89}Zr]Zr-DFO-trastuzumab in NCIN87 tumors on coadministration with statins, in both multiple- and single-dose T-DM1 regimens, indicating that T-DM1 therapy had reduced membrane tumoral HER2 expression at 39 d after therapy initiation (Fig. 2A). Ex vivo biodistribution of the tumors excised from mice after imaging quantified a 1.3-fold decrease in [^{89}Zr]Zr-DFO-trastuzumab uptake when statins were coadministered with T-DM1 compared with T-DM1 administration alone, which was significant in T-DM1 single-dose versus T-DM1/statin single-dose treatment ($P = 0.02$; Fig. 2B; Supplemental Fig. 2). [^{89}Zr]Zr-DFO-trastuzumab tumor uptake on PET images (measured at %ID/g) correlated with tumor volume ($r = 0.97$, $P = 0.03$; Fig. 2C), indicating a positive correlation between trastuzumab-tumor binding and tumor size at 39 d after therapy initiation.

Overall, T-DM1/statin combination therapy significantly reduced membrane HER2 tumoral expression compared with T-DM1 treatment alone, which can be annotated in vivo using immuno-PET.

Statins Enhance the Efficacy of the ADC T-DXd in HER2-Positive Gastric Tumors

Next, we sought to investigate whether including a statin could enhance the efficacy of the trastuzumab ADC T-DXd (*5,6*). T-DXd is showing excellent promise in treating gastric cancer, with initial clinical trials reporting a 51% objective response rate for HER2-positive gastric cancers (*17*). Initially using NCIN87 xenografts, we replicated the single-dose regime such that a single dose of T-DXd was administered at 5 mg/kg along with two doses of lovastatin (4.15 mg/kg) administered 12 h before and on the day of T-DXd administration (Fig. 3A). Both T-DXd and T-DXd/statin treatments reduced tumor volumes over the first 20 d of measurement, but in the next 14 d, T-DXd–treated tumors began to regrow, whereas T-DXd/statin-treated tumors remained controlled, resulting in a significant difference in growth between the two groups ($P = 0.006$; Fig. 3B; Supplemental Figs. 3 and 4). Tumor volume fold-change at 34 d after treatment initiation averaged 0.57 ± 0.09 T-DXd/statin compared with 1.31 ± 0.22 in tumors treated with T-DXd alone ($P = 0.008$; Fig. 3C).

To annotate changes in tumoral HER2 before and at 29 d after T-DXd therapy, we used [^{64}Cu]Cu-NOTA-trastuzumab before and after therapy, as the half-life of copper-64 is 12.7 h, allowing multiple imaging sessions during our therapy window. Additionally, recent studies have shown the ability of ^{64}Cu-labeled trastuzumab to monitor responder versus nonresponder tumors to ADC therapy (*28*). Immuno-PET imaging after therapy in NCIN87 tumors demonstrated a decrease in uptake of [^{64}Cu]Cu-NOTA-trastuzumab in both T-DXd and T-DXd/statin cohorts (Fig. 3D), and the mean %ID/g tumor values from both pretherapy and posttherapy imaging correlated with tumor volume ($r = 0.77$, $P = 0.03$; Supplemental Fig. 5).

Overall, T-DXd therapy was enhanced on coadministration with statins in HER2-positive NCIN87 tumors, and HER2 expression on immuno-PET could be monitored before and after therapy with ^{64}Cu-labeled trastuzumab.

ADC Single-Dose Coadministered with Statins Reduces Tumor Volume in a Trastuzumab-Resistant Gastric PDX Model

Cell-line xenograft models such as NCIN87 cancer cells are commercially available and can be used across multiple analyses for preclinical work. However, they do not always represent the heterogeneity observed in clinical samples. PDX models offer an alternative that can better represent patient tumor tissue and response to therapies (*29*). Gastric PDXs recapitulate patient tumor inter- and intratumoral heterogeneity in histology and genetic characteristics (*30*). Because of the preservation of tumoral heterogeneity, PDXs are thought of as avatars for patients when testing novel therapies (*31*). Therefore, we chose a previously established gastric PDX model with known clinical resistance to anti-HER2 therapy to test both the T-DM1/statin and the T-DXd/statin single-dose regimes (Fig. 4A) (*18,21*).

When the HER2-positive gastric PDX was treated with a single dose of T-DM1/statin (Fig. 4A), tumor volume was significantly reduced ($P < 0.001$) compared with T-DM1 alone and control cohorts (Fig. 4B; Supplemental Fig. 6). The volume fold-change of T-DM1/statin tumors was significantly lower ($P < 0.001$) than for the equivalent T-DM1–alone regime. No significant differences in tumor volume fold-change were observed between T-DM1/statin single-dose and multiple-dose regimes (Fig. 4C). Equally, when

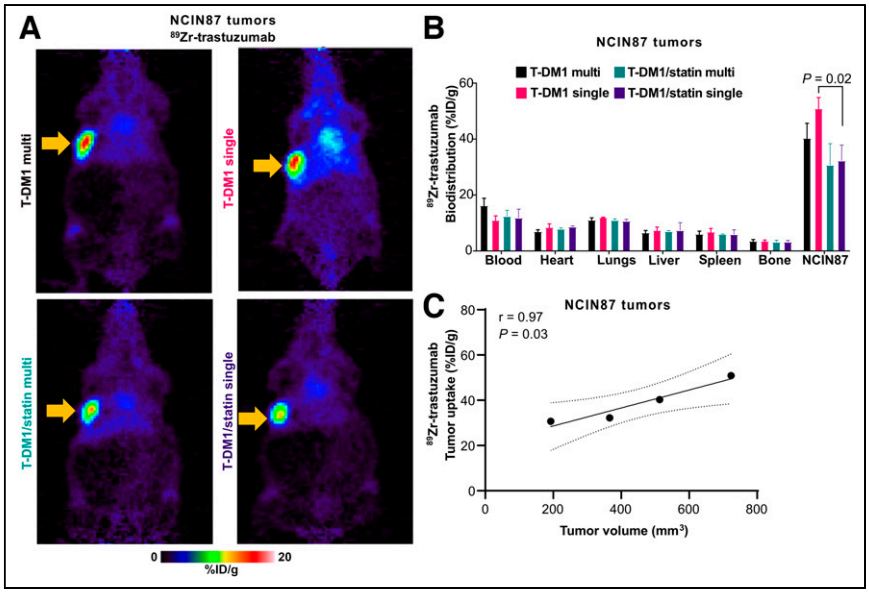

FIGURE 2. (A and B) Representative PET images (A) and biodistribution (B) of [^{89}Zr]Zr-DFO-trastuzumab displaying %ID/g acquired 48 h after radiolabeled trastuzumab injection on day 39 for T-DM1 single-treatment regime, T-DM1/statin single-treatment regime, T-DM1 multiple-treatment regime, and T-DM1/statin multiple-treatment regime. Tumor location is indicated by arrow. Data are mean ± SD (n = 4). Significant P values (<0.05) are displayed for tumor mean comparisons and were calculated by unpaired Student t test. (C) Scatterplot of mean %ID/g of [^{89}Zr]Zr-DFO-trastuzumab in tumor regions against tumor volume (mm^3). Pearson correlation coefficient (r) and P value are displayed. Line of best fit is displayed (solid black line) with 95% CIs (dotted black lines).

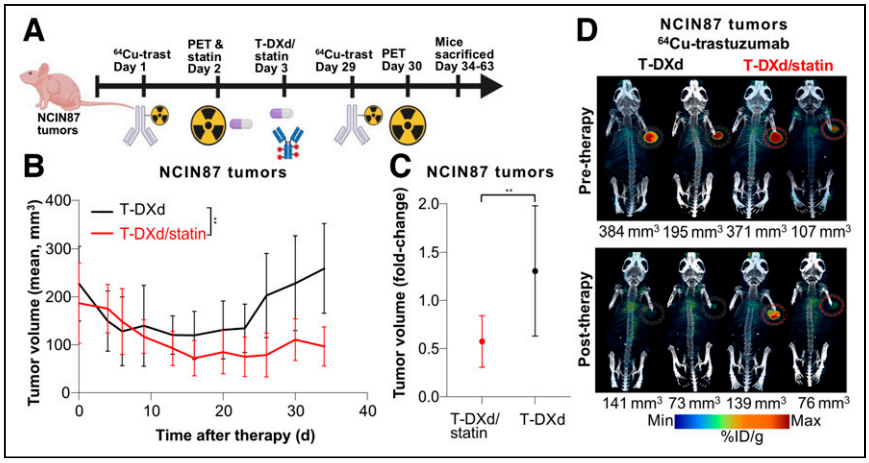

FIGURE 3. (A) Schematic illustrating T-DXd and statin dose administration across single-dose regime. NCIN87 gastric xenografts were established in female nude mice (9 per group). Once tumors reached about 200 mm^3, mice were intravenously administered T-DXd, 5 mg/kg weekly (for 1 wk—single-treatment regime). Lovastatin (4.15 mg/kg) was orally administrated 12 h before and simultaneously with intravenous injection of T-DXd. [^{64}Cu]Cu-NOTA-trastuzumab was intravenously administered on days 1 and 29, and PET images were collected before (day 2) and after (day 30) therapy. Mice were sacrificed 34–63 d after initiating therapy. Schematic was created with Biorender.com. (B) Tumor volumes (mm^3) were measured across 34 d for T-DXd and T-DXd/statin. Mean ± SD of 9 mice per group is shown. $^{**}P$ = 0.006 at endpoint based on 2-way repeated-measures ANOVA. (C) Tumor volume fold-change in NCIN87 tumor volume in T-DXd or T-DXd/statin. Fold-change between days 0 and 34 is displayed as mean ± SD. $^{**}P$ = 0.008 calculated by unpaired Student t test. (D) Representative PET images of [^{64}Cu]Cu-NOTA-trastuzumab displaying %ID/g acquired at 24 h after radiolabeled trastuzumab injection before therapy (day 2) and after therapy (day 30) for T-DXd and T-DXd/statin. Two different mice with varying tumor sizes from 73 to 384 mm^3 are displayed for each group and each time point. Tumors are encircled.

the HER2-positive gastric PDX was treated with a single dose of T-DXd/statin (Fig. 4A), there was a significant ($P < 0.001$) reduction in tumor volume compared with T-DXd alone (Fig. 4D; Supplemental Fig. 7). The tumor volume fold-change of T-DM1/statin PDXs was significantly lower (P = 0.07; Fig. 4E; Supplemental Fig. 8) than for the equivalent T-DXd–alone regime. Finally, both T-DXd single-dose and T-DXd/statin single-dose treatments were more effective at controlling gastric PDX tumor volumes than were the T-DM1 and T-DM1/statin single-dose regimes, as measured by tumor volume fold-change ($P < 0.0001$ for all comparisons; Supplemental Fig. 9).

Overall, both the T-DM1 and the T-DXd/statin single-dose regimes effectively reduced tumor volumes in a clinically representative gastric PDX model in which the originating patient tumor was previously resistant to anti-HER2 therapy.

ADC Therapy *Co*administered with Statin Downregulates HER2 Signaling and Increases DNA Damage

After observations that an ADC/statin single-dose regime is effective at reducing tumor volume and induces alterations in HER2 expression as detected via immuno-PET, we sought to annotate changes in HER2 signaling in total protein extracts once tumor tissue was excised on day 43 after ADC therapy. Western blot analysis of NCIN87 tumor extracts demonstrated depletion of HER2 and phospho-HER2/total HER2 after T-DM1 coadministration with statins, in both multiple- and single-dose regimes (Fig. 5A), with a 15- to 30-fold reduction compared with control tumors and tumors treated with T-DM1 alone (Fig. 5B). Additionally, other HER family receptors, including EGFR and HER3, were depleted in T-DM1/statin groups, with an 8-fold reduction in phospho-HER3/total HER3 and a 6-fold reduction in phospho-EGFR/total EGFR in comparison to control tumors (Figs. 5A and 5B). Tyrosine phosphorylation of multiple proteins was decreased in T-DM1/statin multiple- or single-dose tumors (Fig. 5A). The results shown in Figure 5 were further validated in 2 more independent analyses (Supplemental Figs. 10–13).

In addition to evaluating protein expression in T-DM1–treated tumors, we found that HER2 levels were 6-fold lower and barely detectable in T-DXd and T-DXd/statin-treated tumors harvested at 63 d after therapy induction compared with control tumors (Fig. 5C; Supplemental Fig. 14). Further analyses in NCIN87 cells treated

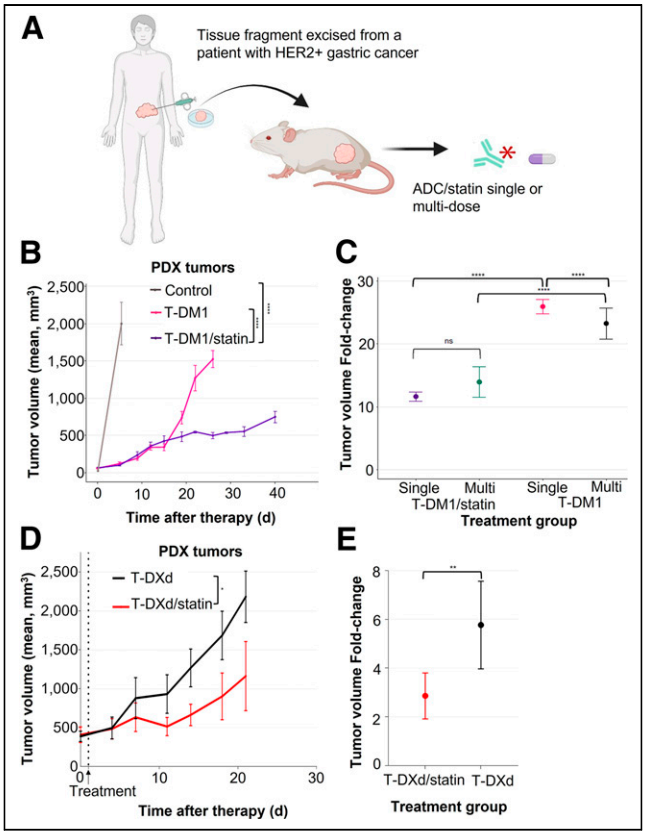

FIGURE 4. (A) Schematic displaying establishment of HER-positive gastric cancer PDX from patient tumor. Tumor fragments were implanted subcutaneously into NSG mice (≥8 per group). T-DM1/statin multiple- and single-dose schedules were administered as described in Figure 1. T-DXd/statin single-dose schedule was administered as described in Figure 3. Schematic was created with Biorender.com. (B) Tumor volumes (mm^3) were measured across 40 d for control, T-DM1 single-dose regime, and T-DM1/statin single-dose regime. Mean ± SD is shown ($n \geq 8$ per group). ****$P < 0.0001$ based on 2-way repeated measures ANOVA. (C) Tumor volume fold-change in gastric PDX for T-DM1 or T-DM1/statin (1 wk of therapy, single-treatment regime) and for T-DM1 or T-DM1/statin (5 wk, multiple-treatment regime reported (*21*)). Fold-change between first and last tumor volume measurements is displayed as mean ± SD ($n \geq 5$ per group). ns = not significant. ****$P < 0.0001$ based on 1-way ANOVA. (D) Tumor volumes (mm^3) were measured across 21 d for T-DXd single-dose regime and T-DXd/statin single-dose regime. Mean ± SD is shown ($n \geq 8$ per group). *$P = 0.02$ based on 2-way repeated measures ANOVA. (E) Tumor volume fold-change in gastric PDX for T-DXd or T-DXd/statin. Fold-change between first and last tumor volume measurements is displayed as mean ± SD ($n \geq 8$ per group). **$P = 0.007$ based on unpaired Student *t* test.

for 48 h with ADC alone or in combination with lovastatin demonstrated a 2- to 6.5-fold reduction in HER2 and a 2- to 3-fold reduction in phospho-HER2 (Fig. 5D; Supplemental Fig. 15). Phosphorylated tyrosines were downregulated in all treatments compared with control (Fig. 5D; Supplemental Fig. 16). Because the DXd chemotherapy is expected to induce DNA damage, expression of H2AX, phosphorylated H2AX, cleaved PARP, and full-length PARP was evaluated at the cellular level. All 4 treatments (T-DM1, T-DM1/statin, T-DXd, and T-DXd/statin) increased the expression of markers for DNA damage, showing a 3- to 6-fold increase in H2AX and a 1.6- to 3.5-fold increase in phosphorylated H2AX compared with control cells (Fig. 5D; Supplemental Fig. 17). Interestingly, levels of H2AX and phosphorylated H2AX were relatively high in T-DM1/statin-treated samples and in T-DXd–treated cells. Finally, the ratio of cleaved PARP/PARP in T-DM1/statin and T-DXd/statin-treated cells was 16-fold and 28-fold higher than in control cells (Fig. 5E; Supplemental Fig. 18), suggesting cleavage of full-length PARP in cells undergoing DNA damage.

Overall, Western blot analyses demonstrated depletion of HER2 and decreased phosphorylation of HER2 and multiple downstream targets on coadministration of T-DM1 or T-DXd with statin compared with control tumors. Additionally, Western blot analyses showed expression of DNA damage markers on acute treatment with HER2-targeting ADC-plus-statin therapies.

DISCUSSION

ADCs have become eminent in oncologic treatment schedules because of their ability to precisely target tumors with potent efficacy. Indeed, 14 ADCs have been approved for cancer treatment, and more than 100 different ADCs are being evaluated in clinical trials (*4*). T-DM1 and T-DXd are two Food and Drug Administration–approved anti-HER2 antibody conjugates, which are based on the antibody trastuzumab linked to a cytotoxic payload. T-DM1 comprises trastuzumab conjugated with a microtubule-targeting payload (DM1), whereas T-DXd contains trastuzumab linked to a topoisomerase-1 inhibitor payload. T-DM1 is effective in treating HER2-positive breast tumors, but in clinical trials it failed to treat HER2-expressing gastric cancers (*15*). Most recently, T-DXd demonstrated improved efficacy in HER2-positive advanced gastric tumors (*17*). A common characteristic of T-DM1 and T-DXd is that treatment schedules often require frequent infusions of the cold ADC to maintain therapy. Although ADCs are usually well tolerated, severe side effects can occur in patients, including low blood counts, liver damage, and lung damage (*32*). After our previous studies showing that cholesterol-depleting drugs (statins) enhance cell-surface HER2 availability (*18*) and ADC internalization (*20*) in ways that enhance anti-HER2 antibody–based therapies, we have now demonstrated here that statins can be used to reduce the number of infusion schedules of the cold ADC. In our studies, preclinical gastric tumors treated with a single dose of T-DM1 in combination with a statin achieve responses similar to multiple doses of T-DM1. Tumor growth inhibition in HER2-positive NCIN87 and PDX gastric tumors was achieved with a single dose of T-DXd, and growth inhibition was enhanced by coadministration with lovastatin.

We found that preclinical immuno-PET with radiolabeled trastuzumab can monitor HER2 tumoral levels on treatment with the T-DM1 or T-DXd. Recently, another study demonstrated the use of HER2 PET to monitor response to T-DM1 therapy in breast cancer mouse models, with a decrease in radiolabeled anti-HER2 antibody observed after treatment (*33*). In metastatic breast cancer patients, pretreatment imaging of HER2 targeting with ^{64}Cu-labeled trastuzumab (*28*) or ^{89}Zr-labeled trastuzumab (*34*) was predictive of treatment response, with higher uptake of radiolabeled antibody before treatment being predictive of a better response. Our current study showed a correlation between the %ID/g of ^{89}Zr-labeled trastuzumab or ^{64}Cu-labeled trastuzumab and volume in tumors treated with T-DM1 or T-DXd, respectively. Our preclinical data contribute to the accumulating evidence that HER2 PET can provide noninvasive insight into receptor tumoral levels.

Tumors of animals treated with T-DM1 or T-DXd plus statin showed growth suppression and demonstrated lower uptake on PET images after therapy. These imaging findings correlated with changes

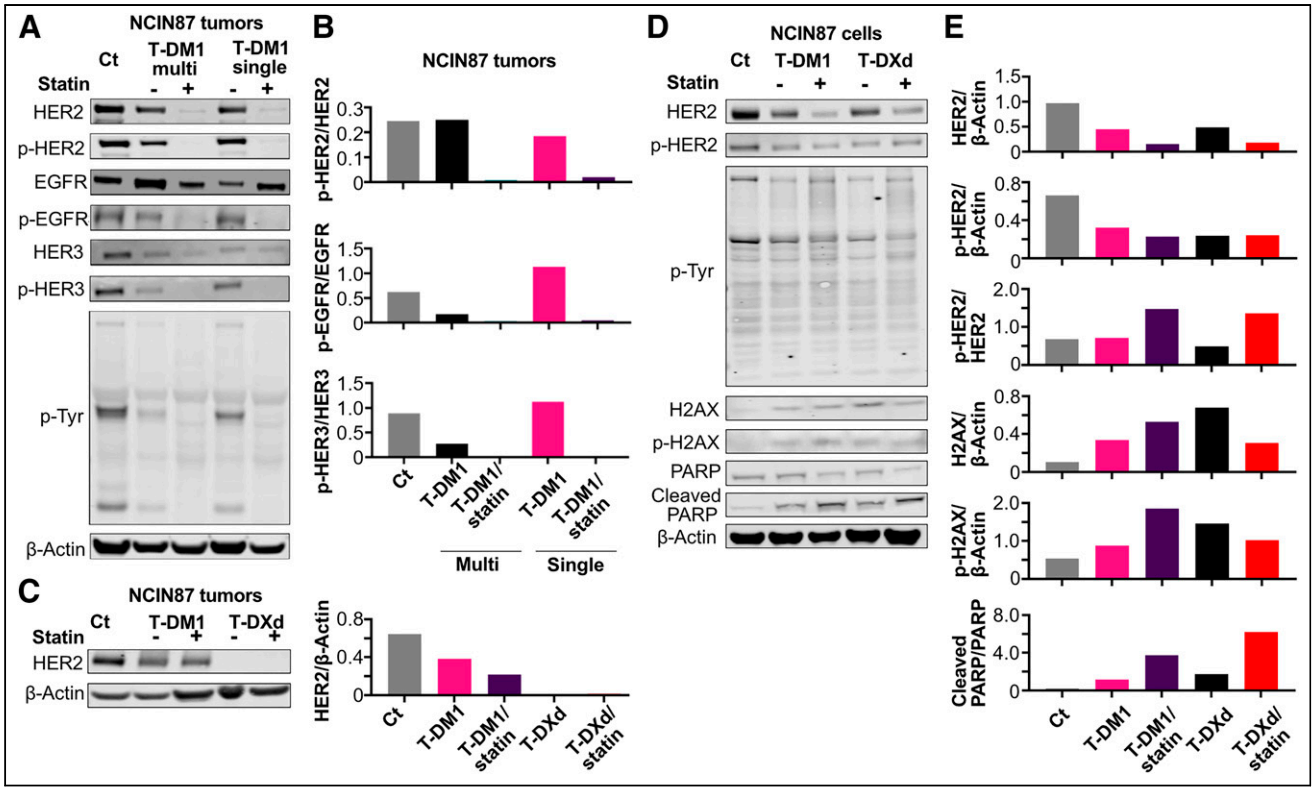

FIGURE 5. (A and B) Western blot analyses (A) and quantification (B) at 43 d after treatment of NCIN87 tumors for control, T-DM1 multiple-treatment regime, T-DM1/statin multiple-treatment regime, T-DM1 single-treatment regime, and T-DM1/statin single-treatment regime. Western blots show expression of proteins in HER2 downstream signaling pathways including HER2, phosphor-HER2, EGFR, phosphor-EGFR, HER3, phosphor-HER3, and phosphor-tyrosine. β-actin was used as loading control. Quantifications shown in B relate to A, and analyses for additional repeats are shown in supplemental materials. (C) HER2 Western blot analyses and quantification after treatment of NCIN87 tumors for control, T-DM1 single-treatment regime, T-DM1/statin single-treatment regime, T-DXd single-treatment regime, and T-DXd/statin single-treatment regime. β-actin was used as loading control. (D) Western blot analyses and (E) quantification for NCIN87 cells treated with vehicle, T-DM1, T-DM1/statin, T-DXd, and T-DXd/statin for 48 h. Western blots show expression of HER2, phosphor-HER2, phosphor-tyrosine, H2AX, phosphor-H2AX, cleaved PARP, and PARP. β-actin was used as loading control. Full membranes of all repeats are shown in supplemental materials. p-Tyr = phosphor-tyrosine.

in HER2 and HER2-mediated signaling in tumors, because we observed—by Western blot analyses—decreased HER2, HER2 phosphorylation, and phosphor-tyrosine phosphorylation in tumors. HER2 phosphorylation results in signaling activation, and further downstream phosphorylation of multiple proteins occurs, ultimately resulting in increased proliferation, survival, and migration of cancer cells that are driven by HER2 signaling (*35,36*). Our results indicate a suppression in HER-mediated signaling after T-DM1/statin and T-DXd/statin therapy.

Anti-HER2 ADC efficacy depends on a series of several sequential events: binding of the ADC to the cell-surface HER2, ability of the antibody to decrease HER2-mediated oncogenic signaling and to induce antibody-mediated cellular toxicity, ADC-HER2 internalization, and, finally, payload release inside the tumor cell (*37–39*). Our previous preclinical experiments are consistent with the hypothesis that surface-localized HER2s can be modulated to enhance trastuzumab and T-DM1 efficacy (*18,21*). Therefore, pharmacologic strategies that augment HER2 antibody tumor binding and further internalization may allow reducing the number of dose schedules of the therapeutic antibody or ADC. We observed that treating tumors with T-DM1 in combination with lovastatin enhances T-DM1 tumor binding and internalization in vitro, resulting in higher efficacy than with T-DM1 alone (*21*). Importantly, our results show that just a single dose of T-DM1/statin is efficacious in gastric tumor models and was just as effective as multiple doses of T-DM1/statin in a PDX gastric model (Fig. 4). Overall, our findings support a mechanism by which stabilization of membrane HER2 increases anti-HER2 ADC binding; consequently, internalization is enhanced, which in our studies allowed a lower number T-DM1 doses to achieve therapeutic efficacy in mice. If translated to the clinic, this strategy could potentially reduce the number of doses of T-DM1 and adverse events associated with T-DM1 treatment (*40*).

Although T-DM1 and T-DXd are composed of the same antibody (trastuzumab), several differences exist between these two ADCs: T-DXd has a higher drug-to-antibody ratio than T-DM1, two different linkers are used in the preparation of T-DM1 and T-DXd, the two cytotoxic payloads DM1 and DXd have a different mechanism of action, and DXd permeability allows for a bystander effect to the neighbor cells regardless of their expression for HER2. Coadministration of statin with an ADC enhanced the expression of the DNA damage markers PARP and H2AX. Additionally, PARP and H2AX were expressed in T-DM1/statin-treated cells but not in cells treated with T-DM1 alone, indicating induction of DNA damage with statins. Indeed, lipophilic statins such as lovastatin have previously been reported to sensitize cancer cells to radiotherapy via increased DNA damage. However, statins are also reported to protect against DNA damage in normal tissues by increasing DNA

double-strand break repair (*23,41*). This mechanism of action by statins requires further investigation with other preclinical tumor models.

In addition to modulating HER2 in tumors, it is possible that statins might also induce alterations in other HER2-expressing nontumor organs. Since trastuzumab does not bind the rodent homolog of HER2 (*42*), our study failed to address the effects of statin in trastuzumab binding to HER2-expressing murine tissues. Additionally, the pleiotropic effects of statins suggest that lovastatin has potential off-target effects in addition to HER2 modulation, none of which were determined in our study.

CONCLUSION

Our results showed that immuno-PET with radiolabeled trastuzumab can monitor HER2 tumoral levels on treatment with HER2-targeted ADCs in preclinical models. Our study also demonstrated that the combination of a statin with anti-HER2 ADC enhances therapeutic efficacy in preclinical HER2-expressing gastric tumor models in ways that allow reducing the number of ADC therapeutic doses. Considering that statins are prescribed to millions of people every year to reduce cholesterol levels (*43*), our findings have the potential to be translated to clinical trials to test the feasibility, safety, and efficacy of using statins in combination with HER2-targeting ADCs.

DISCLOSURE

The MSK Anti-Tumor Assessment Core and Molecular Cytology Core Facility is supported by NIH grant P30 CA08748. Abbey Zidel's contributions to the research were supported through Washington University's biology undergraduate research program (Bio 200/500) and MIR Summer Research Program. This research was supported by internal funds provided by the Mallinckrodt Institute of Radiology and the NIH (R01 CA244233-01A1). Patrícia Pereira acknowledges the NIH (R01 CA244233-01A1), American Cancer Society (IRG-21-133-64-03), Cancer Research Foundation (P22-03203), Elsa Pardee Foundation, Alvin J. Siteman Cancer Center through the Foundation for Barnes–Jewish Hospital, and National Cancer Institute (P30 CA091842). Jason Lewis acknowledges NIH NCI R35 CA232130 and NIH R01 CA244233-01A1. The Preclinical Imaging Facility at Washington University School of Medicine in St. Louis was supported by NIH/NCI Siteman Cancer Center support grant P30CA091842, NIH instrumentation grants S10OD018515 and S10OD030403, and internal funds provided by the Mallinckrodt Institute of Radiology. No other potential conflict of interest relevant to this article was reported.

ACKNOWLEDGMENTS

We thank the Washington University isotope production team for producing copper-64, and we thank the small-animal imaging facility for helping with small-animal PET/CT data generation. We also acknowledge the MSK Small-Animal Imaging Core Facility, the MSK Radiochemistry and Molecular Imaging Probe Core, and the MSK Anti-Tumor Assessment Core and Molecular Cytology Core Facility. We are grateful to Dr. Elisa De Stanchina and the entire team at the Antitumor Assessment Core at MSK for helping with the PDX models. We are thankful to Dr. Luis Batista for letting us use the Odyssey Infrared Imaging System. We thank Dr. Luke Carter for his help with the 3D Slicer software. We gratefully acknowledge the Siteman Cancer Center pharmacy for providing us with trastuzumab/Herceptin, T-DM1/Kadcyla (Genentech), and T-DXd/Enhertu (Daiichi Sankyo) antibodies.

KEY POINTS

QUESTION: Can HER2-targeted immuno-PET inform on the tumor response and dose regime of ADC therapy in combination with statins?

PERTINENT FINDINGS: Immuno-PET serves as a noninvasive tool to monitor HER2 depletion in vivo in response to T-DM1, T-DXd, T-DM1/statin, or T-DXd/statin administration.

IMPLICATIONS FOR PATIENT CARE: The enhanced potency of ADC therapy observed on coadministration with statins can be monitored with immuno-PET and enables lowering of ADC doses while achieving similar efficacy.

REFERENCES

1. Hudis CA. Trastuzumab: mechanism of action and use in clinical practice. *N Engl J Med.* 2007;357:39–51.
2. Modi S, Saura C, Yamashita T, et al. Trastuzumab deruxtecan in previously treated HER2-positive breast cancer. *N Engl J Med.* 2020;382:610–621.
3. Modi S, Saura C, Yamashita T, et al. Abstract PD3-06: updated results from DESTINY-breast01, a phase 2 trial of trastuzumab deruxtecan (T-DXd) in HER2 positive metastatic breast cancer [abstract]. *Cancer Res.* 2021;81(suppl):PD3-06.
4. Fu Z, Li S, Han S, Shi C, Zhang Y. Antibody drug conjugate: the "biological missile" for targeted cancer therapy. *Signal Transduct Target Ther.* 2022;7:93.
5. Ferraro E, Drago JZ, Modi S. Implementing antibody-drug conjugates (ADCs) in HER2-positive breast cancer: state of the art and future directions. *Breast Cancer Res.* 2021;23:84.
6. do Pazo C, Nawaz K, Webster RM. The oncology market for antibody-drug conjugates. *Nat Rev Drug Discov.* 2021;20:583–584.
7. Diéras V, Miles D, Verma S, et al. Trastuzumab emtansine versus capecitabine plus lapatinib in patients with previously treated HER2-positive advanced breast cancer (EMILIA): a descriptive analysis of final overall survival results from a randomised, open-label, phase 3 trial. *Lancet Oncol.* 2017;18:732–742.
8. Tarantino P, Carmagnani Pestana R, Corti C, et al. Antibody–drug conjugates: smart chemotherapy delivery across tumor histologies. *CA Cancer J Clin.* 2022;72:165–182.
9. Mamounas EP, Untch M, Mano MS, et al. Adjuvant T-DM1 versus trastuzumab in patients with residual invasive disease after neoadjuvant therapy for HER2-positive breast cancer: subgroup analyses from KATHERINE. *Ann Oncol.* 2021;32:1005–1014.
10. Iqbal N, Iqbal N. Human epidermal growth factor receptor 2 (HER2) in cancers: overexpression and therapeutic implications. *Mol Biol Int.* 2014;2014:852748.
11. Oh D-Y, Bang Y-J. HER2-targeted therapies: a role beyond breast cancer. *Nat Rev Clin Oncol.* 2020;17:33–48.
12. Li BT, Smit EF, Goto Y, et al. Trastuzumab deruxtecan in HER2-mutant non–small-cell lung cancer. *N Engl J Med.* 2022;386:241–251.
13. Grillo F, Fassan M, Sarocchi F, Fiocca R, Mastracci L. HER2 heterogeneity in gastric/gastroesophageal cancers: from benchside to practice. *World J Gastroenterol.* 2016;22:5879–5887.
14. Bang Y-J, Van Cutsem E, Feyereislova A, et al. Trastuzumab in combination with chemotherapy versus chemotherapy alone for treatment of HER2-positive advanced gastric or gastro-oesophageal junction cancer (ToGA): a phase 3, open-label, randomised controlled trial. *Lancet.* 2010;376:687–697.
15. Thuss-Patience PC, Shah MA, Ohtsu A, et al. Trastuzumab emtansine versus taxane use for previously treated HER2-positive locally advanced or metastatic gastric or gastro-oesophageal junction adenocarcinoma (GATSBY): an international randomised, open-label, adaptive, phase 2/3 study. *Lancet Oncol.* 2017;18:640–653.
16. Janjigian YY, Viglianti N, Liu F, Mendoza-Naranjo A, Croydon L. A phase Ib/II, multicenter, open-label, dose-escalation, and dose-expansion study evaluating trastuzumab deruxtecan (T-DXd, DS-8201) monotherapy and combinations in patients with HER2-overexpressing gastric cancer (DESTINY-Gastric03) [abstract]. *J Clin Oncol.* 2021;39(suppl):TPS261.
17. Shitara K, Bang Y-J, Iwasa S, et al. Trastuzumab deruxtecan in previously treated HER2-positive gastric cancer. *N Engl J Med.* 2020;382:2419–2430.

18. Pereira PMR, Sharma SK, Carter LM, et al. Caveolin-1 mediates cellular distribution of HER2 and affects trastuzumab binding and therapeutic efficacy. *Nat Commun.* 2018;9:5137.
19. Filho OM, Viale G, Stein S, et al. Impact of HER2 heterogeneity on treatment response of early-stage HER2-positive breast cancer: phase II neoadjuvant clinical trial of T-DM1 combined with pertuzumab. *Cancer Discov.* 2021;11:2474–2487.
20. Orr G, Hu D, Ozçelik S, Opresko LK, Wiley HS, Colson SD. Cholesterol dictates the freedom of EGF receptors and HER2 in the plane of the membrane. *Biophys J.* 2005;89:1362–1373.
21. Pereira PMR, Mandleywala K, Monette S, et al. Caveolin-1 temporal modulation enhances antibody drug efficacy in heterogeneous gastric cancer. *Nat Commun.* 2022;13:2526.
22. Guruswamy S, Rao CV. Synergistic effects of lovastatin and celecoxib on caveolin-1 and its down-stream signaling molecules: implications for colon cancer prevention. *Int J Oncol.* 2009;35:1037–1043.
23. Fritz G, Henninger C, Huelsenbeck J. Potential use of HMG-CoA reductase inhibitors (statins) as radioprotective agents. *Br Med Bull.* 2011;97:17–26.
24. Valentovic M. Lovastatin. Lovastatin. In: Enna SJ, Bylund DB, eds. *xPharm: The Comprehensive Pharmacology Reference.* Elsevier; 2007:1–5.
25. Pondé N, Ameye L, Lambertini M, Paesmans M, Piccart M, de Azambuja E. Trastuzumab emtansine (T-DM1)-associated cardiotoxicity: pooled analysis in advanced HER2-positive breast cancer. *Eur J Cancer.* 2020;126:65–73.
26. Abdel-Qadir H, Bobrowski D, Zhou L, et al. Statin exposure and risk of heart failure after anthracycline- or trastuzumab-based chemotherapy for early breast cancer: a propensity score–matched cohort study. *J Am Heart Assoc.* 2021;10:e018393.
27. Woo S-K, Jang SJ, Seo M-J, et al. Development of ^{64}Cu-NOTA-trastuzumab for HER2 targeting: a radiopharmaceutical with improved pharmacokinetics for human studies. *J Nucl Med.* 2019;60:26–33.
28. Mortimer JE, Bading JR, Frankel PH, et al. Use of ^{64}Cu-DOTA-trastuzumab PET to predict response and outcome of patients receiving trastuzumab emtansine for metastatic breast cancer: a pilot study. *J Nucl Med.* 2022;63:1145–1148.
29. Choi SYC, Lin D, Gout PW, Collins CC, Xu Y, Wang Y. Lessons from patient-derived xenografts for better in vitro modeling of human cancer. *Adv Drug Deliv Rev.* 2014;79–80:222–237.
30. Corso S, Isella C, Bellomo SE, et al. A comprehensive PDX gastric cancer collection captures cancer cell–intrinsic transcriptional MSI traits. *Cancer Res.* 2019;79:5884–5896.
31. Zeng M, Pi C, Li K, et al. Patient-derived xenograft: a more standard "Avatar" model in preclinical studies of gastric cancer. *Front Oncol.* 2022;12:898563.
32. Wolska-Washer A, Robak T. Safety and tolerability of antibody-drug conjugates in cancer. *Drug Saf.* 2019;42:295–314.
33. Massicano AVF, Lee S, Crenshaw BK, et al. Imaging of HER2 with [^{89}Zr]pertuzumab in response to T-DM1 therapy. *Cancer Biother Radiopharm.* 2019;34:209–217.
34. Gebhart G, Lamberts LE, Wimana Z, et al. Molecular imaging as a tool to investigate heterogeneity of advanced HER2-positive breast cancer and to predict patient outcome under trastuzumab emtansine (T-DM1): the ZEPHIR trial. *Ann Oncol.* 2016;27:619–624.
35. Arienti C, Pignatta S, Tesei A. Epidermal growth factor receptor family and its role in gastric cancer. *Front Oncol.* 2019;9:1308.
36. Roviello G, Aprile G, D'Angelo A, et al. Human epidermal growth factor receptor 2 (HER2) in advanced gastric cancer: where do we stand? *Gastric Cancer.* 2021;24:765–779.
37. Drago JZ, Modi S, Chandarlapaty S. Unlocking the potential of antibody–drug conjugates for cancer therapy. *Nat Rev Clin Oncol.* 2021;18:327–344.
38. Ogitani Y, Aida T, Hagihara K, et al. DS-8201a, a novel HER2-targeting ADC with a novel DNA topoisomerase I inhibitor, demonstrates a promising antitumor efficacy with differentiation from T-DM1. *Clin Cancer Res.* 2016;22:5097–5108.
39. Junttila TT, Li G, Parsons K, Phillips GL, Sliwkowski MX. Trastuzumab-DM1 (T-DM1) retains all the mechanisms of action of trastuzumab and efficiently inhibits growth of lapatinib insensitive breast cancer. *Breast Cancer Res Treat.* 2011;128:347–356.
40. Kowalczyk L, Bartsch R, Singer CF, Farr A. Adverse events of trastuzumab emtansine (T-DM1) in the treatment of HER2-positive breast cancer patients. *Breast Care (Basel).* 2017;12:401–408.
41. Efimova EV, Ricco N, Labay E, et al. HMG-CoA reductase inhibition delays DNA repair and promotes senescence after tumor irradiation. *Mol Cancer Ther.* 2018;17:407–418.
42. Lewis Phillips G, Guo J, Kiefer JR, et al. Trastuzumab does not bind rat or mouse ErbB2/neu: implications for selection of non-clinical safety models for trastuzumab-based therapeutics. *Breast Cancer Res Treat.* 2022;191:303–317.
43. Juarez D, Fruman DA. Targeting the mevalonate pathway in cancer. *Trends Cancer.* 2021;7:525–540.